ADVANCES IN GEODESY AND GEOINFORMATION
(formerly GEODESY AND CARTOGRAPHY)
Vol. 73, no. 2, article no. e55, 2024

https://doi.org/10.24425/agg.2024.150684

Original paper

Displacements study of a dam using low-cost GNSS receivers, high precision leveling and Finite Element Model

Rosendo Romero-Andrade[1]*, Manuel Edwiges Trejo-Soto[1], Luis Enrique Acosta-González[2], Daniel Hernández-Andrade[1], Karan Nayak[1], Vivian Hernández-Columbie[2], Richard Serrano-Agila[3], Yedid Guadalupe Zambrano-Medina[1]

[1]Autonomous University of Sinaloa, Sinaloa, Mexico
e-mail: r.romero11@info.uas.edu.mx; ORCID: http://orcid.org/0000-0003-3786-0576

e-mail: mtrejosoto@uas.edu.mx; ORCID: http://orcid.org/0000-0002-5028-2849

e-mail: daniel.hernandezan@gmail.com; ORCID: http://orcid.org/0000-0001-6544-4460

e-mail: nayakkaran.facite@uas.edu.mx; ORCID: http://orcid.org/0000-0002-5015-402X

e-mail: yedidzambrano@uas.edu.mx; ORCID: http://orcid.org/0000-0001-8820-0688

[2]University of Holguín, Holguín, Cuba
e-mail: luis.acosta.glez@gmail.com; ORCID: http://orcid.org/0000-0002-2723-9850

e-mail: vivianhc86@gmail.com; ORCID: http://orcid.org/0000-0003-1989-2427

[3]Particular Technical University of Loja, Loja, Ecuador
e-mail: rgserrano@utpl.edu.ec; ORCID: http://orcid.org/0000-0003-1765-4126

*Corresponding author: Rosendo Romero-Andrade, e-mail: r.romero11@info.uas.edu.mx

Received: 2024-01-24 / Accepted: 2024-07-12

Abstract: Emerging low-cost Global Navigation Satellite System (GNSS) receivers are gaining prominence in geosciences and surveying engineering, finding application in diverse positioning research endeavors. The primary aim of this study was to assess the structural integrity using low-cost GNSS technology, whose usability has advanced significantly. The fundamental premise of the research is the assumption that the lifespan of the dam has reached its end in accordance with international regulations. Over a span of four years and across multiple campaigns, a combination of low-cost GNSS, high precision leveling data, and Finite Element Modeling techniques were employed to monitor deformations at the Sanalona dam. A notable deformation was identified at the central curtain of the dam. Utilizing low-cost GNSS equipment, horizontal deformations of up to 10 cm and vertical deformations of up to 30 cm were recorded. These values do not jeopardize the operational objectives of the dam as per the stipulations of the U.S. Army Corps of Engineers (USACE). The Sanalona Dam continues to operate effectively within the bounds of international regulations, even when subjected to extraordinary phenomena. The findings of this study hold relevance for the wider adoption

of low-cost GNSS equipment in civil engineering structures and other demanding geodetic applications, including historic infrastructures. Moreover, the study underscores the viability of conducting precise dam surveys utilizing low-cost GNSS devices in campaign mode.

Keywords: FEM, GNSS, monitoring, dam, low-cost GNSS

1. Introduction

Geodesy encompasses the systematic observation of structural distortions in diverse types of constructions. An indispensable structure in this context, with pivotal implications for water supply, flood management, agriculture, and hydroelectric power, is a dam. Surveillance of dams is crucial to avert potential failures, stemming from factors like land erosion, water load, hydraulic gradients, and water saturation (Kalkan, 2014). The repercussions of dam failure are profound, encompassing substantial economic and human losses. Given the multifaceted role that dams play in various sectors, including their impact on ecosystems and surrounding communities, it becomes imperative to underscore the importance of continuous observation and preventive measures. By closely monitoring and addressing potential issues such as structural weaknesses and environmental changes, we can mitigate the risks associated with dam failures, safeguarding both the infrastructure and the well-being of those dependent on it. The synergy between geodesy and dam surveillance thus emerges as a critical component in ensuring the resilience and sustainability of vital water-related systems. When comparing large dams to other engineering structures, factors such as air and water temperature, water level, pressure, uplift, and rock deformability reveal a more pronounced correlation with environmental, hydraulic, and geomechanical influences. All these factors can impact the structural behavior of the dam (Yigit et al., 2016).

Geodetic measurements have become a widely employed approach for the surveying and continuous monitoring of dam stability. Numerous investigations, as exemplified by Guler et al. (2006), have incorporated both geodetic and geotechnical methodologies to track horizontal and vertical displacements over extended timeframes. The collected data underwent analysis through numerical techniques, demonstrating a commendable alignment with geodetic measurements. Researchers such as Bayrak (2008) and Gikas and Sakellariou (2008) formulated a model to scrutinize the correlation between reservoir level and dam deformation, revealing a robust relationship between the two variables. In a study by Ehiorobo and Irughe-Ehigiator (2015), the efficacy of GPS in measuring horizontal displacements was underscored, particularly through differential methods, proving effective even in detecting subtle displacements. Yigit et al. (2016) carried out a correlation analysis investigating the relationship between periodic and linear responses in dam displacement and seasonal temperature variations, along with the linear increase in reservoir levels. Their findings indicated that Finite Element Model (FEM) analysis had the capability to predict deformations accurately. Similarly, Acosta-González et al. (2018) delved into the displacement of earth fill dams using a combination of high-precision leveling and GPS methods, along with a numerical model. Their study highlighted the

significance of these methods in monitoring both horizontal and vertical displacements. In a related context, Gu et al. (2022) introduced a method designed to eliminate significant errors and predict the behavior of concrete dams. However, they emphasized the need for further research to enhance structural health monitoring capabilities.

Geodetic-grade GNSS receivers have traditionally been the standard in geodetic studies. However, a recent development is the emergence of low-cost GNSS equipment that offers similar features but at significantly reduced prices compared to their geodetic-grade counterparts. These affordable GNSS receivers, typically priced around $200 US, stand in stark contrast to geodetic receivers that can cost approximately $US16,000.00 (Zamora-Maciel et al., 2020; Romero-Andrade et al., 2021a). This significant cost difference has opened up opportunities to explore new methodologies and applications where lower-cost equipment may be suitable. The initial evaluations of low-cost GNSS receivers focused on mapping purposes. Studies conducted by Sioulis et al. (2015) and Tsakiri et al. (2017, 2018) demonstrated that these low-cost receivers yielded comparable outcomes to RTK positioning achieved with geodetic receivers, particularly in benign environments. This underscores the potential of low-cost GNSS receivers to provide cost-effective solutions without compromising the quality of results in certain applications. Various approaches have been used with low-cost GNSS receivers. Hohensinn et al. (2022) demonstrated the impact of different multi-band antenna types, including geodetic medion-grade helical-type, patch-type and low-cost helical antenna, with this experiment they reach a one cm of precision with PPP method. Cina and Piras (2015) proposed land monitoring with relative static method using mass-market GNSS receivers and demonstrated the possibility of achieving millimeter accuracy under appropriate operational conditions. Similarly, Poluzzi et al. (2019) showed the capability of low-cost GNSS receivers to detect slow displacement with high precision and real-time solutions for early warning purposes. They found these devices were suitable for monitoring structures and could achieve millimeter-level accuracy. Romero-Andrade et al. (2019) conducted a comparative analysis of Precise Point Positioning (PPP) using different technologies and emphasized the accuracy achieved with RTKLIB in various environments. Garrido-Carretero et al. (2019) demonstrated low-cost GNSS receivers had horizontal and vertical uncertainties close to 5.5 mm and 11 mm, respectively, indicating their comparable positioning performance to survey-grade receivers in real-time positioning for short baselines, making them a feasible option in geomatics. Additional investigations by Hamza et al. (2020) have further the ZED-F9P with u-blox ANN-MB-00 antenna was investigate its potential for displacement detection. The results, obtained on a basis of 30-min sessions show that low-cost GNSS instruments can detect displacements from 10 mm upwards with a high level of reliability. Similarly, Tunini et al. (2022) used low-cost devices for crustal deformation purposes, they show that mm-order precision can be achieved with cost-effective GNSS receivers, and the obtained results are comparable to those obtained using high-precise geodetic receivers in a long time series. Wielgocka et al. (2021) show that horizontal accuracy was achieved with Precise Point Positioning (PPP) if a session is extended to at least 2.5 hr. Romero-Andrade et al. (2021b) delved into the exploration of Precise Point Positioning (PPP) and static relative methods for processing data in challenging environments, emphasizing the significance of sampling rates in achieving high precision. In recent studies, Zhao et al.,

(2022) conducted tests using low-cost GNSS receivers on bridge structures, introducing a novel approach for real-time cable deformation monitoring, specifically in a suspension bridge. The results revealed that the measured error on bridge towers using low-cost GNSS equipment was below 0.005 m horizontally and 0.008 m vertically, as compared to a robotic total station. This suggests the potential use of low-cost GNSS receivers in structural health monitoring. Vázquez-Ontiveros et al., (2022) undertook a study on the Sanalona dam, monitoring local deformations and reservoir water levels through GPS observations from a Continuous GPS (CGPS) station over 3.5 years, they identified deformations in the dam crest at rates of -0.77 mm/yr, -9.95 mm/yr, and 1.62 mm/yr in the East, North, and Up components, respectively. In a more recent study (Vázquez-Ontiveros et al., 2023), the same dam's risk was evaluated using the same CGPS station, alongside Synthetic Aperture Interferometric Radar and Finite Element Modeling. The estimated maximum dam crest displacement was 7.3 mm and 6.7 mm.

In general, GNSS technology has been used for decades to monitor the structural deformations in various constructions, including dams. Its viability becomes clearer when the outcomes from new low-cost technology are correlated with results obtained through other methodologies such as Finite Element Method (FEM) and high precision leveling. The primary aim of the research is to showcase the potential of low-cost GNSS receivers in understanding the behavior of Sanalona dam, aligning with regulations set forth by the United States Army Corps of Engineers Structural Deformation Surveying (EM 1110-2-1009) (Structural Deformation Surveying, 2018). To achieve this objective, the study employed both low-cost and geodetic GNSS receivers, high precision leveling, and Finite Element Method analysis. A fundamental assumption underlying the research is that the dam's expected lifetime has reached its conclusion based on international regulations. The paper's structure is delineated as follows: Section 1 provides an introduction and describes the study area, Section 2 outlines the utilized data and methods, Section 3 presents the obtained results, Section 4 engages in discussions and correlations, and finally, Section 5 encapsulates the conclusions drawn from the study.

Study case: Sanalona dam

The Sanalona dam, situated along the Tamazula River in Culiacan de Rosales, Sinaloa, Mexico (Fig. 1), is a significant infrastructure built between 1940 and 1948 (CONAGUA, 2022). It serves as a crucial irrigation resource, covering an expansive area of 60,000 hectares, while also contributing to electricity generation. With a total height of 81 meters, the dam's key dimensions include a bed height of 63 meters, a crown length stretching 1,031 meters, and a base length of 415 meters. Its slopes vary, with the upstream slope at 3:1 and the downstream slope at 2:1. Additionally, the dam features three sidewalks: two 4-meter-wide sidewalks positioned at elevations of 148.34 meters and 131.67 meters respectively, and a third 6-meter-wide sidewalk located at an elevation of 115 meters.

The dam structure comprises a soil-type curtain, consisting of an impermeable core flanked by an asymmetrically permeable layer made of gravel and sand. To prevent wave erosion, the upstream slope is protected by a layer of rock, while the impermeable core primarily relies on underlying granite bedrock for support. During construction, a trench of 10-meter depth was excavated, with the impermeable core and permeable materials resting on riverbed sediments composed of gravel and sand.

The curtain dam is segmented into three distinct zones:

1. The first zone consists of a waterproof core formed by combining two different types of banks. The "Cordon de Lomas" bank, situated approximately 1 kilometer upstream of El Tlacuache dam, comprises well-graded gravel with minimal fines and incorporates a clay layer to enhance surface material quality. The second bank, "Tucuruguay", composed of altered granite clay, is positioned roughly 2.5 kilometers upstream from the curtain dam and was used to a lesser extent, primarily in lower sections. Material compaction involved the use of two types of rollers: smooth rollers weighing 20 tons were predominantly used to compact 0.20-meter thickness increments. The impervious core features a 2:1 upstream slope and a 1.5:1 downstream slope.
2. The second zone includes permeable supports made predominantly from gravel, sand obtained from nearby riverbeds, and excavated material to accommodate excess material. This mixture was compacted by adding water and rolling it smooth. The berms within this zone, positioned at different elevations, measured 4 meters and 6 meters respectively, all finished with a 1.5:1 slope.
3. The third zone comprises quarry material in the form of a rock sheet located downstream, serving as the unloading channel for excavation activities. This rock sheet, with a thickness of one meter, is placed solely on the upstream slope.

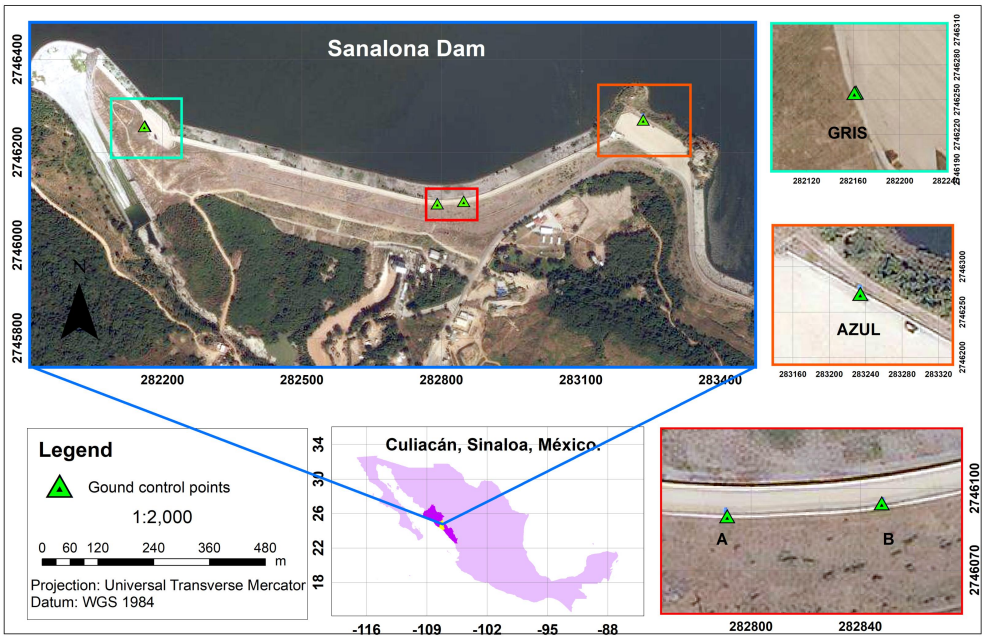

Fig. 1. Sanalona dam location

2. Material and methods

2.1. Displacement analysis of GPS observations

As per USACE standards outlined in Kalkan (2014) and (Structural Deformation Surveying (EM 1110-2-1009), 2018), specific accuracy requirements are established for structure target points. In the context of monitoring concrete arch dams, achieving an accuracy within ±5 to ±10 mm is mandated for long-term horizontal displacement, while vertical displacement necessitates an accuracy within ±2 mm. Conversely, rock fill dams demand a broader range, with monitoring specifications dictating an accuracy range of ±20 to ±30 mm for horizontal displacement and ±10 mm for vertical displacement. For data analysis, general movement trends are described using a point displacement d_n:

$$d_n(\Delta_x, \Delta_y, \Delta_z), \tag{1}$$

where for n means point number.

Point displacements are calculated by taking difference between adjusted coordinates obtained during most recent survey campaign (l) and coordinates obtained at reference time (i):

$$\Delta_x = x_l - x_i, \tag{2}$$

$$\Delta_y = y_l - y_i, \tag{3}$$

$$\Delta_z = z_l - z_i. \tag{4}$$

In this context, coordinates displacement is represented by x, y, and z. Each movement vector possesses both magnitude and direction, expressed as point displacement coordinates differences. These vectors show displacement fields within a specific time interval. If the displacement exceeds expected movement under normal operational conditions, it suggests a potential abnormal behavior. By comparing calculated magnitude displacement with its associated accuracy, it is possible to determine if reported movement is likely attributable to survey errors:

$$|d_n| < (e_n), \tag{5}$$

$$|d_n| = \sqrt{\left(\Delta x^2 + \Delta y^2 + \Delta z^2\right)}, \tag{6}$$

$$e_n = (1.96) \cdot \sqrt{\left(\sigma_l^2 + \sigma_f^2\right)}. \tag{7}$$

In this context, d_n represents magnitude displacement; e_n denotes combined 95% confidence ellipse maximum dimension point. σ_l refers final position standard error; and σ_f represents initial position standard error. In other words, the measured displacement (vertical and horizontal) carried out in campaigns will be taken as an actual movement "$|d_n|$", if the measured displacement exceeds the expected movement "(e_n)" under normal operating conditions, it will indicate a possible abnormal situation.

2.2. Finite Element Model

It's increasingly crucial to conduct experiments at a real scale and under authentic conditions to ensure precise results for numerical methods (Szostak-Chrzanowski, 2006). In this study, a comparison was drawn between vertical and horizontal displacement data obtained through geodetic methods like GNSS positioning. Deterministic analysis was carried out using a Finite Element Model (FEM), utilizing the Geostudio SIGMA/W module 2012 (Brier and Jayanti, 2020).

For the FEM analysis, the primary section of the Sanalona dam curtain was chosen, specifically focusing on the crown and berm slope control points in lower water areas (CONAGUA, 2022). The FEM modeling primarily concentrated on static deformation and meticulously considered various aspects such as geometry, construction stages encompassing fill placement and deposit filling, which played significant roles in the modeling process. The models incorporated fundamental material characteristics, including interfaces between layers, and specific boundary conditions were applied based on the research case. Water load conditions were defined in accordance with piezometric lines to enable pore pressure computation. Figure 2 illustrates the material and section utilized for the Sanalona dam modeling, comprising three layers of soil. The core was compacted using waterproof material, while the filter and transition layers were constituted of gravel and sand materials. The foundation incorporated a composite material with a granite bedrock component (Table 1). This data are used for modeling deformations when a significant displacement is detected which may be close to or exceed the established tolerance limits in the standards. The location where the displacements occur need to be observed and the loads and the type of soil that are supporting the structure need to be analyzed.

Table 1. Sanalona dam curtain soil characteristics which are also utilized in Arenoso Dam, Cordoba, Spain (Acosta-González et al., 2018), and in Sanalona dam (Vázquez-Ontiveros et al., 2023)

Soil (layer)	Material type	Material properties				
		E·103 (kN/m^2)	ν	γ (kN/m^3)	C (kN/m^2)	φ_0
1	Nucleus (compacted waterproof material)	1350	0.25	23	15	35
2	Filter and transition (gravel and sand)	200	0.30	22.0	–	42
3	Foundation (granite bedrock)	8400	0.20	26	–	–

It's noteworthy that the soil characteristics used for the Sanalona dam in Mexico share similarities with those applied in the Arenoso dam in Cordoba, Spain, as highlighted by Acosta-González et al. (2018). Consequently, similar soil characteristics were adopted for the modeling purposes, aligning with findings from Vázquez-Ontiveros et al. (2023) as well.

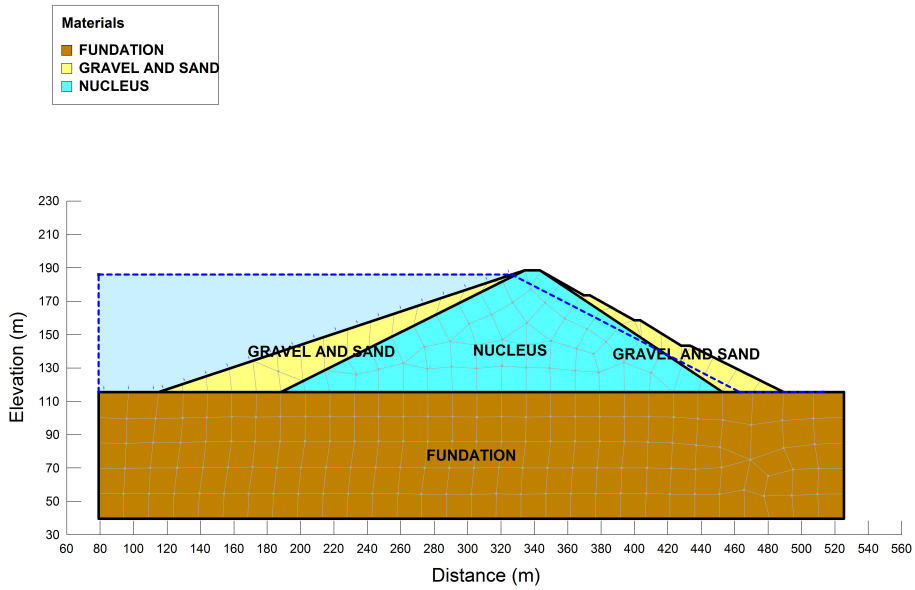

Fig. 2. Typical section commonly employed for geotechnical analysis and modeling

2.3. High precision leveling, GNSS data acquisition and processing

Fourteen GNSS campaigns were conducted between October 4, 2019, and November 12, 2022, to monitor horizontal displacements. Continuous or periodic monitoring couldn't be consistently maintained due to challenges related to conducting surveys in private areas. Nevertheless, the monitoring accounted for significant events such as hurricanes and earthquakes that occurred in the Sinaloa State during this timeframe (Table 2). For the months of September and October, the reservoir fill level exceeds more than 100%, this needs to be considered for the proper interpretation of the displacements and the settlement of the dam.

On October 4, 2019, an initial campaign was conducted utilizing GNSS geodetic receivers placed on all pillars to establish reference coordinates. Subsequent campaigns utilized two GEOMAX ZENITH25 GNSS receivers positioned at GRIS and AZUL points. Additionally, two low-cost GNSS receivers were employed at points A and B within the middle section of the Sanalona dam, chosen for an anticipated higher displacement.

The low-cost receivers consisted of a C099-F9P application board with ZED-F9P and an ASTECH701975.01A model geodetic order antenna (depicted in Fig. 3B), situated at points A and B. The control of the low-cost GNSS receivers was managed through a laptop running U-Center software (Ublox, 2022). All collected data was initially stored in "ubx" format and then converted to RINEX format using RTKLib (Takasu, 2013) software. The low-cost GNSS receivers were configured with a 0.2 s (5 Hz) sampling rate due to observation losses, similarly, the data was decimated to 30 seconds using CSRS-PPP software. According the Romero-Andrade (2021a) low-cost devices tend to

Table 2. Survey date and reservoir level obtained from National Water Commission (CONAGUA) in Mexico. Notably, an "Orlene" hurricane and a "Kay" tropical rain event occurred on September 07 and 14, 2022, respectively

Date	Reservoir fill (%)
October 4, 2019	51.52
December 2, 2019	87.58
June 23, 2020	7.74
September 5, 2021	75.18
October 8, 2021	100.01
November 5, 2021	54.46
March 4, 2022	54.46
March 24, 2022	43.16
April 8, 2022	35.37
June 30, 2022	22.33
September 10, 2022	100.14
October 8, 2022	100.14
November 12, 2022	87.70

loose observations derived from some offset in the internal clock, this affect directly the integrity and the precise positioning, nevertheless, with extended time (more than 30 minutes), the high precision at high frequencies can be achieved. The Precise Point Positioning (PPP) Hofmann-Wellenhof et al. (2008) method was used. PPP is commonly preferred technique in surveying structures due to its attainable accuracy, as referenced in Kaloop et al. (2020) and Xue et al. (2022). It has also found application in seismic event detection, as noted in Martín et al. (2015). One of the primary advantages of PPP over the Static Relative method is its independence from nearby reference stations, allowing for standalone operation (Teunissen, 2020). Notably, even low-cost GNSS receivers have been successfully employed for PPP applications (Manzini et al., 2022). Studies by Tétreault et al. (2005) suggest that processing data at rates higher than 30 seconds in static mode PPP does not necessarily improve solution accuracy and can even reduce it for short datasets. In the same way, according to Bojorquez-Pacheco et al. (2023) it is recommendable the use of the geodetic grade antenna in combination with low-cost GNSS to obtain high precision. During observations, a cut-off angle of 7.5°was set to ensure a clear surrounding environment around the geodetic-grade antennas. Each observation session lasted for 4 hours. According to Choy et al. (2017), a general rule for PPP-static solutions indicates that 60 minutes are sufficient for convergence to achieve a horizontal accuracy of 5 cm. However, Chen et al. (2021) proposed that convergence time might be shorter, depending on satellite orbits, clock corrections, and bias products from the satellites and receivers used.

The GNSS observations underwent processing utilizing CSRS-PPP software (Tétreault et al., 2005) and Precise Point Positioning with Ambiguity Resolution (PPP-AR) (Pan et

al., 2017). Various inputs such as code and phase observables, International GNSS Service (IGS) precise satellite orbits (Colombo, 1986), CLK-RINEX satellite products, Saastamoinen troposphere model (Saastamoinen, 1973), relativistic effects correction (Kouba, 2015), receiver antenna phase center corrections from IGS antex file (igs14_2247.atx, https://files.igs.org/pub/station/general/), and phase wind-up effects (Wu et al., 1992) were accounted for. Solid earth tide corrections were included (Luzum and Petit, 2010), with the International Terrestrial Reference Frame (ITRF) serving as the observation reference frame. For vertical displacement measurements, high precision leveling techniques were employed during survey campaigns conducted on August 18, 2018, March 11, 2022 and September 12, 2022. The leveling process utilized a LEICA DNA03 digital level and a 3-meter invar bar-coded staff (Fig. 3A). The primary objective was to monitor settlement at the crest dam, focusing on the AZUL stable point (Fig. 3C), situated at the highest point of the dam where the structure is supported on the hilltop. These surveys aimed to determine relative vertical displacements of control points.

Fig. 3. Equipment used: a)Geodetic GNSS receiver (GEOMAX ZENITH25), b)DNA-03 Leica level, c)Low-cost GNSS receiver, model ZED F9P with antenna ASTECH701975.01A

3. Results

3.1. Displacements using low cost GNSS receivers

Throughout all the campaigns, displacements were computed, encompassing horizontal, horizontal-vertical, and vertical components (Table 3). The displacement data from the campaign executed on October 4, 2019, was utilized as a reference point for analysis. An ENU system was employed to analyze the coordinates from the low-cost GNSS receivers, which revealed three distinct displacements: (a) a 3D displacement in both directions, (b) a horizontal displacement, and (c) a vertical displacement.

Observations indicated a one-centimeter displacement during periods when the reservoir was filled to less than 90% capacity (Table 3). However, once the reservoir reached full capacity, the calculated displacement exceeded 10 centimeters in most points. Notably, points A and B exhibited the highest deformation within the middle curtain,

consistent with measurements derived from InSAR as observed in Vázquez-Ontiveros et al. (2023). On March 4, 2022, a floating solution was obtained using a low-cost GNSS receiver, initially indicating lower deformation. However, when the reservoir was abruptly filled to 100%, the deformation increased up to 15 centimeters. The low-cost GNSS receivers consistently showcased displacement, which notably intensified during the rainy season when the reservoir was filled. Initial displacements were observed in September, October, and November 2022, attributed to a sudden increase in reservoir fill from 22.33% to 100%.

Research conducted on April 8, 2022, highlighted that GRIS and AZUL points exhibited greater deformations compared to points A and B. This variation could be attributed to differences in reservoir fill timing. The directions of displacements resembled those calculated by Acosta-González et al. (2018) when the reservoir was filled (100%). However, when the reservoir fill was less than 80%, the displacement exhibited a rearrangement.

Table 3. All campaigns displacements according to USACE regulations obtained with a low-cost GNSS receivers. ND: no data

Date	Point	E (m)	N (m)	U (m)	Displacement			Fill of the reservoir (%)
					3D (m)	Horizontal (m)	Vertical (m)	
December 2, 2019	A	0.023	0.008	–0.089	0.052	0	0	87.58
	B	0.004	–0.021	–0.242	0.197	0	0.211	
	GRIS	0.011	0.015	–0.098	0.086	0	0	
	AZUL	ND	ND	ND	ND	0	0	
June 23, 2020	A	0.010	–0.005	0.179	0.052	0	0	7.74
	B	0.007	–0.004	–0.240	0.216	0	0.299	
	GRIS	0.036	0.017	–0.046	0.017	0.009	0	
	AZUL	–0.001	0.009	0.074	0	0	0	
September 5, 2021	A	0.011	–0.016	–0.068	0	0	0	75.18
	B	0.012	0.001	–0.266	0.244	0.002	0.324	
	GRIS	0.010	0.020	–0.097	0.063	0.074	0.023	
	AZUL	0.007	0.024	0.009	0.024	0	0	
October 8, 2021	A	0.027	–0.003	–0.070	0.049	0.007	0.002	100
	B	0.006	–0.015	–0.264	0.242	0	0.296	
	GRIS	0.001	0.020	–0.073	0.034	0	0	
	AZUL	0.010	0.006	0.18	0.127	0	0.111	
November 5, 2021	A	0.014	–0.012	–0.100	0.078	0	0.050	54.46
	B	0.013	–0.015	–0.278	0.259	0.002	0.324	
	GRIS	–0.001	0.021	–0.111	0.076	0	0.052	
	AZUL	–0.007	0.015	0.01	0.028	0	0	

Continued on next page

Table 3 – *Continued from previous page*

Date	Point	E (m)	N (m)	U (m)	Displacement			Fill of the reservoir (%)
					3D (m)	Horizontal (m)	Vertical (m)	
March 4, 2022	A	0.005	0.006	0.013	0	0	0	54.46
	B	0.677	–0.238	–1.394	12.905	0	0	
	GRIS	0.015	0.002	0.178	0.049	0	0.016	
	AZUL	0.009	0.022	0.033	0.004	0	0	
March 24, 2022	A	ND	ND	ND	0.074	ND	ND	43.16
	B	0.001	–0.080	0.243	2.634	0	0	
	GRIS	–0.002	0.005	–0.078	0.049	0	0.012	
	AZUL	ND	ND	ND	0	0	0	
April 8, 2022	A	0.004	0.021	0.171	0.119	0	0	35.37
	B	0.001	0.011	0.030	0.030	0	0	
	GRIS	ND	ND	ND	ND	ND	0	
	AZUL	–0.128	0.029	0.026	0.078	0.095	0	
June 30, 2022	A	–0.009	0.008	0.149	0.141	0	0.108	22.33
	B	–0.009	–0.001	–0.090	0.155	0	0	
	GRIS	–0.002	0.026	–0.016	0.001	0.001	0.023	
	AZUL	–0.027	0.030	0.111	0.070	0.001	0.023	
September 10, 2022	A	0.134	–0.078	–0.078	0.152	0.130	0.003	100
	B	0.144	–0.072	–0.001	0.140	0.144	0	
	GRIS	0.148	–0.074	–0.103	0.161	0.041	0.006	
	AZUL	0.137	–0.041	0.002	0.095	0.107	0	
October 8, 2022	A	0.129	–0.078	–0.107	0.152	0.129	0.003	100
	B	0.127	–0.097	–0.122	0.171	0.139	0.071	
	GRIS	0.133	–0.075	–0.104	0.086	0.041	0.006	
	AZUL	0.111	–0.056	–0.008	0.080	0.091	0	
November 12, 2022	A	0.142	–0.084	0.105	0.128	0.129	0	87.7
	B	0.060	–0.061	–0.050	0.823	0	0	
	GRIS	0.151	–0.093	–0.122	0.185	0.151	0.072	
	AZUL	0.126	–0.061	–0.008	0.093	0.104	0	

The most substantial displacements were noted during the rainy season in September, October, and November 2022. In the east component, deformations reached 16 centimeters on average, with a horizontal component averaging around 10 centimeters. Concerning the vertical component, there was a settlement of 26 centimeters (excluding the float solution

of point B found on March 4, 2022). However, it's important to note that the vertical component, due to its lower precision, might not accurately represent the displacement, as indicated in Hamza et al. (2021), Janos and Kuras (2021), Romero-Andrade et al. (2021b).

The analysis, in adherence to USACE regulations, encompassed both horizontal and vertical components. The horizontal component exhibited the most substantial deformation in the central part of the dam, reaching 16 centimeters when the dam was rapidly filled due to meteorological phenomena during the rainy season (as detailed in Table 3). According to Engomoen et al. (2014) and Structural Deformation Surveying (EM 1110-2-1009) (2018), the dam did not surpass the recommended values established in its design. Regarding the vertical component, a settlement of 30 centimeters was initially detected, which appeared larger than expected. However, it's essential to consider that the GNSS vertical component tends to be less precise (Hofmann-Wellenhof et al., 2008), making the deformations identified using low-cost GNSS less reliable. Consequently, precise leveling observations were conducted instead.

According to precise leveling calculations, no significant settlement in the dam was detected. There was minimal difference observed between August 2019 and September 2022, with the variance tending to remain consistent or similar (Table 4). However, a negative difference was observed in the leveling direction.

Table 4. High precision leveling results

Date	From	To	Level's difference (m)
August 2019	AZUL	GRIS	0.02788
March 2022	AZUL	GRIS	0.02885
September 2022	GRIS	AZUL	–0.02630

The investigation focused on establishing a spatial-temporal correlation between reservoir filling and total horizontal displacement, necessitating the aggregation of individual displacements to derive a single magnitude for comparison with reservoir fill and extreme events data (Fig. 4). Initially, at the onset of 2020, displacements remained minimal even when the reservoir reached its full capacity. However, a notable displacement was observed on September 5, 2021, coinciding with the reservoir reaching its full capacity. Furthermore, the occurrence of Hurricane Orlene on September 7, 2022, resulted in a sudden increase in reservoir filling from 22.33% to 100%. Similarly, a tropical rain event on September 14, 2022, led to the overflow of the dam reservoir. These events exhibited a direct correlation with the observed displacements, highlighting a clear association between extreme events and the recorded displacements. The outcomes underscore the capability of low-cost receivers in detecting even minor displacements.

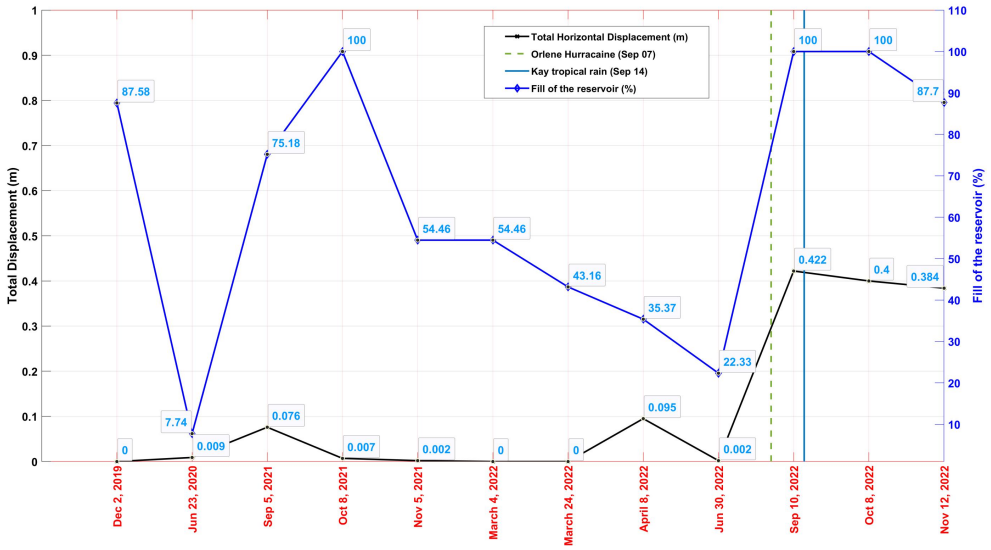

Fig. 4. Total displacements with reservoir filling and meteorological events

3.2. Stresses, deformations, settlements, and horizontal displacements calculations was performed using a Finite Element Method (FEM) model

A FEM model was constructed to maximum water level (MWL) capacity estimate, and its results were compared to observations obtained with low-cost GNSS receivers. This comparison let derivation of water pore pressure and load-deformation models, which are showed in Figure 5 and Figure 6.

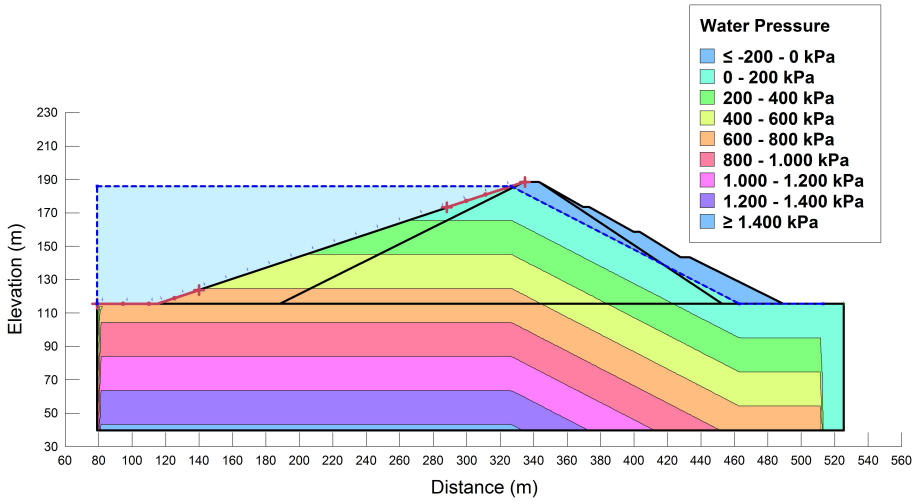

Fig. 5. Steady-state pore water pressure model for Maximum Water Level (MWL)

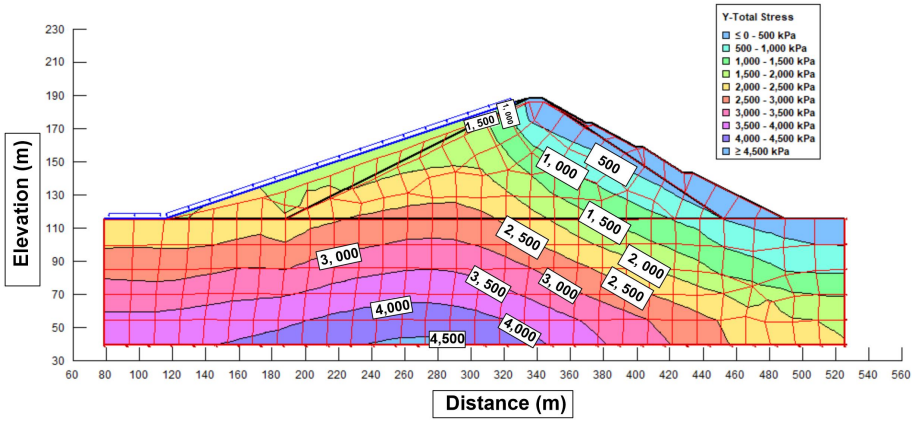

Fig. 6. Load-deformation model for typical section

Displacements were gauged across various segments within different areas of the dam, encompassing the crown, nucleus, and specific berm directions. These displacements were subsequently compared with the observed results obtained from GNSS low-cost receivers. Notably, the dam crown exhibited the most significant settlement, measuring 10 centimeters, which gradually diminished towards the foundation or bedrock. The foundation is characterized by a robust layer of resilient granite, depicted in Figure 7 and Figure 8.

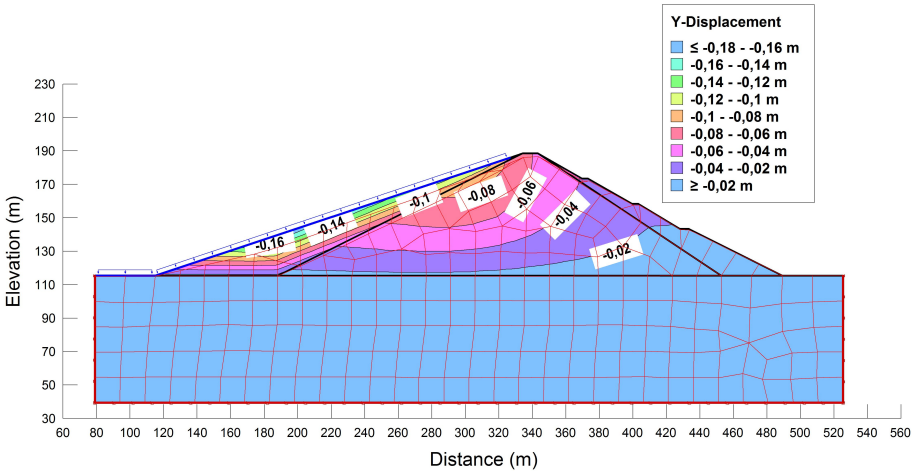

Fig. 7. Crest and berms settlements across typical section

Vertical displacements in the downstream berm were limited to a maximum of 4 cm, whereas the upstream berm saw vertical displacements reaching up to 16 cm, particularly at the foot slope. This aligns with the areas experiencing the highest concentration of stresses exerted by the water column. Upstream slope exhibited maximum horizontal displacements of 6 cm, correlating with the zones bearing the highest stress concentration. In contrast, the downstream slope averaged around 2 cm in horizontal displacement.

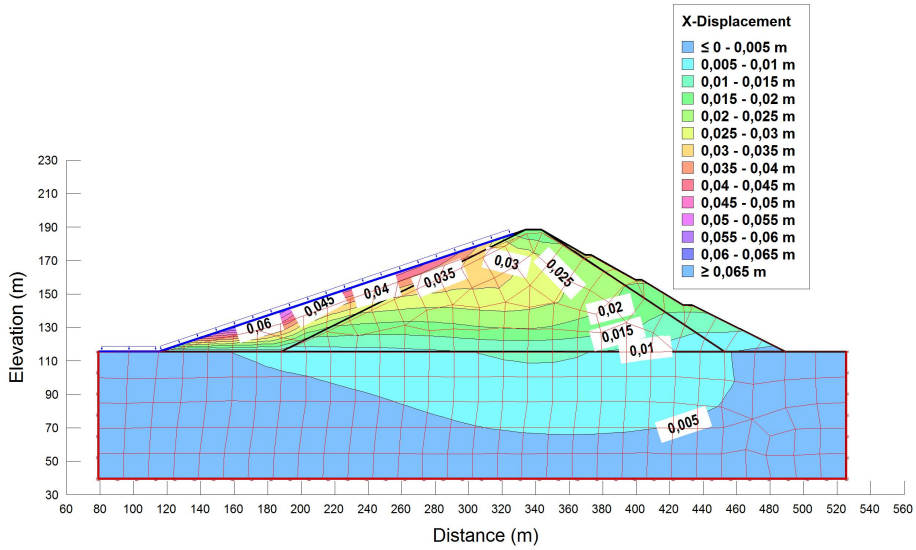

Fig. 8. Load-deformation model for typical section

Discrepancies emerged between the results obtained from geotechnical modeling and those derived from geodetic measurements. The difference between them ranged from 0.002 to 0.004 times the height of the dam (81 m). This variance falls within the range established by international experiences and current regulations (Engomoen et al., 2014; Structural Deformation Surveying (EM 1110-2-1009), 2018). The most considerable difference of 16 cm was observed in the upstream slope berm. Notably, this alignment between the two methods becomes more precise as geodetic monitoring approaches the final phase of soil consolidation.

4. Comparative analysis and discussion

Dams play a crucial role globally by storing large volumes of water for various societal needs and human consumption. Consequently, numerous studies have been undertaken to monitor the behavior of different types of dams. Among these, the Sanalona dam holds significant importance in Sinaloa due to its proximity to the capital city. A study conducted by Vázquez-Ontiveros et al. (2023) showcased the stability of the Sanalona dam through the application of two techniques: InSAR and mathematical modeling, aimed at assessing the risk associated with the dam-reservoir system. Utilizing the InSAR technique with MT-InSAR measurements and employing Sentinel data and SARPROZ software, the analysis was conducted. For the FEM model, the researchers considered the mechanical and physical properties of the Sanalona dam material. Furthermore, horizontal displacements and comparisons were made using a Continuous GPS (CGPS) station located near the curtain, albeit not on the crest, as these CGPS stations were primarily instrumented for seismic monitoring purposes, spanning approximately four years of

data. Their findings revealed that the middle section of the curtain exhibited higher displacements, with maximum radial displacements of 12.4 mm detected with InSAR, 6.7 mm with FEM, and 7.3 mm with GPS. Similarly, in Vázquez-Ontiveros et al. (2022), the same CGPS was employed to analyze displacements, revealing crest displacements of approximately ±5 mm, ±4.5 mm, and ±10 mm in the North, East, and Up components, respectively. Notably, both studies identified the maximum displacement occurring in the middle section of the curtain at the crest.

According to our experimental findings, points A and B, situated at the midpoint of the curtain, are most significantly impacted by variations in reservoir levels. These outcomes have been corroborated by prior research. Our observations indicate that when the reservoir level is below 90%, even a centimeter displacement can be discerned in the horizontal component using low-cost devices. Similarly, during gradual or abrupt reservoir filling to full capacity, horizontal displacements can be detected by low-cost GPS, demonstrating the capability of low-cost GPS with the PPP technique to identify deformations in campaign mode. Additionally, based on the FEM model, greater deformations were observed at points GRIS and AZUL compared to those detected by low-cost GPS. These discrepancies stem from variations in the timing of reservoir filling. Nonetheless, displacements at points GRIS and AZUL were observed to coincide with the onset of the rainy season, mirroring similar deformations detected by low-cost devices.

In accordance with the current state-of-the-art, the vertical component is not recommended for geodetic and low-cost GPS measurements due to its inherent lack of precision, which may not accurately reflect displacements. Therefore, it was imperative to conduct high-precision leveling from stable points to all points along the curtain. Our analysis reveals larger vertical displacements at points A and B in the middle of the curtain, as indicated by low-cost GPS measurements (refer to Table 3). However, it is noteworthy that the vertical component appears to be the most affected when using a low-cost device. Similarly, the results obtained from high-precision leveling remain consistent (as shown in Table 4), aligning with the finite element model (refer to Fig. 7), which illustrates high displacements (e.g., 0.08 m at points GRIS and B) at the crest where observations were conducted.

All deformations on Sanalona dam were determined using GNSS low-cost equipment and compared with reservoir fill level and FEM. Results showed a difference between deformations calculated with FEM and local deformations, which could be attributed to material variations used in FEM model calculations. This difference joins with Acosta-González et al., (2018) conclusions and it is associated with simplifications and assumptions made during FEM modeling process. Also, these discrepancies impact settlement obtained from high-pressure leveling observations. Similarly, geodetic control points were anchored on structure superficial layer, which is evidenced on horizontal displacements observed at points A and B over dam crest. However, geodetic and FEM results tend to line up as soon geodetic monitoring approaches to soil consolidation final phase.

The Horizontal deformations where critical points A and B are positioned on dam middle curtain are in accordance with results to Vázquez-Ontiveros et al. (2023). Other results demonstrate using low-cost GNSS viability, since significant deformation points correspond to those estimated using InSAR by Vázquez-Ontiveros et al. (2023) even with

the absence of in situ geodetic observations, as the CGPS station was not situated on the dam crest. Additionally, these points correlate with reservoir fill level, and even minor deformations can be detected. Overall, Sanalona dam shows signs of stability over time, even after extreme events, like horizontal displacements and reservoir correlation shows.

5. Conclusions

The study employed three methodologies to monitor both horizontal and vertical movements at Sanalona dam. The results validate the effectiveness of employing low-cost GNSS receivers to detect displacements at the dam crest in campaign mode using the Precise Point Positioning (PPP) technique. Notably, horizontal deformations were predominantly observed in the central region of the curtain, consistent with findings from other techniques such as InSAR, as documented by various researchers. The displacements identified by low-cost GNSS receivers, spanning from 2019 to 2022 and ranging in millimeters, consistently support prior research. Interestingly, these receivers demonstrated their capability to detect horizontal movements particularly during rapid reservoir filling caused by extreme events.

A comparison of vertical and horizontal displacements derived from geotechnical modeling with geodetic observations conforms to international standards (0.002-0.004 times the height of the dam). The most significant disparity, amounting to 16 centimeters, was observed in the upstream slope berm. It is expected that as the geodetic method progresses towards the final phase of floor consolidation, this disparity will likely diminish. According to regulations by the U.S. Army Corps of Engineers (USACE), horizontal displacements remain within acceptable limits even during extreme events like hurricanes and tropical rains. Remarkably, the Sanalona dam exhibits a propensity for stability in its horizontal components during similar events. The study underscores the effectiveness of employing campaign mode and low-cost GNSS receivers for monitoring dam behavior. However, it emphasizes the necessity of employing high-precision leveling or satellite technologies for monitoring the vertical component due to its precision constraints.

Author contributions

Conceptualization: M.E.T.S., L.E.A.G., R.R.A.; methodology: M.E.T.S., L.E.A.G., R.R.A., RSA; formal analysis and investigation: D.H.A., V.H.C, Y.G.Z.M; writing – original draft preparation: R.R.A, K.N., L.E.A.G, V.H.C.; writing – review and editing: K.N., D.H.A., M.E.T.S; supervision: M.E.T.S., R.R.A., L.E.A.G.; data curation: D.H.A., V.H.C., Y.G.Z.M; visualization: K.N.

Data availability statement

The datasets used during the concurrent study are available from corresponding author on reasonable request.

Acknowledgements

Authors would like to express their gratitude to anonymous reviewers for their valuable contributions, which greatly enhanced this work quality. This research received support from Autonomous University of Sinaloa under PROFAPI project number PRO_A1_027 and CONAHCYT. Also, the authors are grateful to students (Lizbeth G. Santiago-Sánchez, María F. Castelo-Pimientel, Rafaela M. Llanes-Hernández, Francisco A. Núñez-Espinoza, and Jesús A. Lagunas-Vargas) who help to perform the observations for the experiment.

References

Acosta-González, L.E., de Lacy-Pérez de los Cobos, M.C., Ramos, I. et al. (2018). Displacements Study of an Earth Fill Dam Based on High Precision Geodetic Monitoring and Numerical Modeling. *Sensors*, 18(1369). DOI: 10.3390/s18051369.

Bayrak, T. (2008). Verifying pressure of water on dams, a case study. *Sensors*, 8(9), 5376–5385. DOI: 10.3390/s8095376.

Bojorquez-Pacheco, N., Romero-Andrade, R., Trejo-Soto, M.E. et al. (2023). Performance evaluation of single and double-frequency low-cost GNSS receivers in Static Relative mode. *Geodetski Vestnik*, 67(2), 244–257. DOI: 10.15292/geodetski-vestnik.2023.02.235-248.

Brier, J., and Jayanti, L.D. (2020). *Stress-Strain Modeling with GeoStudio*. Vol. 21, Issue 1.

Chen, C., Xiao, G., Chang, G. et al. (2021). Assessment of GPS/Galileo/BDS Precise Point Positioning with Ambiguity Resolution Using Products from Different Analysis Centers. *Remote Sens.*, 13(16), 3266. DOI: 10.3390/rs13163266.

Choy, S., Bisnath, S., and Rizos, C. (2017). Uncovering common misconceptions in GNSS Precise Point Positioning and its future prospect. *GPS Solut.*, 21(1), 13–22. DOI: 10.1007/s10291-016-0545-x.

Cina, A., and Piras, M. (2015). Performance of low-cost GNSS receiver for landslides monitoring: test and results. *Geomat. Nat. Hazards Risk*, 6(5–7), 497–514. DOI: 10.1080/19475705.2014.889046.

Colombo, O.L. (1986). Ephemeris errors of GPS satellites. *Bulletin Géodésique*, 20706, 64–84.

CONAGUA. (2022). Memoria descriptiva de la Presa Sanalona.

Ehiorobo, J.O., and Irughe-Ehigiator, R. (2015). Monitoring for Horizontal Movement in an Earth Dam Using Differential GPS Monitoring for Horizontal Movement in an Earth Dam Using Siberian State Academy of Geodesy, Novosibirsk , Russia. *J. Emerg. Trends in Eng. Appl. Sci.*, 2, 908–913.

Engomoen, B., Witter, D., Knight, K. et al. (2014). *Chapter 9: static deformation analysis phase 4*. In Design Standars No. 13: Embankment Dams (Reclamatio, p. 126). US Department of Interior: Bureau of Reclamation.

Garrido-Carretero, M.S., de Lacy-Pérez de los Cobos, M.C., Borque-Arancón, M.J. (2019). Low-cost GNSS receiver in RTK positioning under the standard ISO-17123-8: A feasible option in geomatics. *Measurement: J. Int. Measurement Confederation*, 137, 168–178. DOI: 10.1016/j.measurement.2019.01.045.

Gikas, V., and Sakellariou, M. (2008). Settlement analysis of the Mornos earth dam (Greece): Evidence from numerical modeling and geodetic monitoring. *Eng. Struct.*, 30(11), 3074–3081. DOI: 10.1016/j.engstruct.2008.03.019.

Gu, C., Wang, Y., Gu, H. et al. (2022). A Combined Safety Monitoring Model for High Concrete Dams. *App. Sci.*, 12(12103), 1–17. DOI: 10.3390/app122312103.

Guler, G., Kilic, H., Hosbas, G. et al. (2006). Evaluation of the movements of the dam embankments by means of geodetic and geotechnical methods. *J. Surv. Eng.*, 132(1), 31–39. DOI: 10.1061/(ASCE)0733-9453(2006)132:1(31).

Hamza, V., Stopar, B., and Ambrožic, T. (2020). Testing Multi-Frequency Low-Cost GNSS Receivers for Geodetic Monitoring Purposes. *Sensors*, 20, 16. DOI: 10.3390/s20164375.

Hamza, V., Stopar, B., and Sterle, O. (2021). Testing the performance of multi-frequency low-cost gnss receivers and antennas. *Sensors*, 21(6), 1–16. DOI: 10.3390/s21062029.

Hofmann-Wellenhof, B., Lichtenegger, H., and Wasle, E. (2008). *GNSS Global Navigation Satellite System GPS, GLONASS, Galileo and more*. Springer Wien: New York.

Hohensinn, R., Stauffer, R., Glaner, M.F. et al. (2022). Low-Cost GNSS and Real-Time PPP: Assessing the Precision of the u-blox ZED-F9P for Kinematic Monitoring Applications. *Remote Sens.*, 14(20), 1–25. DOI: 10.3390/rs14205100.

Janos, D., and Kuras, P. (2021). Evaluation of Low-Cost GNSS Receiver under Demanding Conditions in RTK Network Mode. *Sensors*, 21. DOI: 10.3390/s21165552.

Kalkan, Y. (2014). Geodetic deformation monitoring of Ataturk Dam in Turkey. *Arab. J. Geosci.*, 7(1), 397–405. DOI: 10.1007/s12517-012-0765-5.

Kaloop, M.R., Yigit, C.O., Dindar, A.A. et al. (2020). Evaluation of the high-rate GNSS-PPP method for vertical structural motion. *Surv. Rev.*, 52(371), 159–171. DOI: 10.1080/00396265.2018.1534362.

Kouba, J. (2015). *A Guide to using international GNSS Service (IGS) Products*. International GNSS Service.

Luzum, B., and Petit, G. (2010). IERS Technical Note, No. 36.

Manzini, N., Orcesi, A., Thom, C. (2022). Performance analysis of low-cost GNSS stations for structural health monitoring of civil engineering structures. *Struct. Infrastruct. Eng.*, 18(5), 595–611. DOI: 10.1080/15732479.2020.1849320.

Martín, A., Anquela, A.B., Dimas-Pagés, A. et al. (2015). Validation of performance of real-time kinematic PPP. A possible tool for deformation monitoring. *Measurement: J. Int. Measurement Confederation*, 69, 95–108. DOI: 10.1016/j.measurement.2015.03.026.

Pan, Z., Chai, H., and Kong, Y. (2017). Integrating multi-GNSS to improve the performance of precise point positioning. *Adv. Space Res.*, 60(12), 2596–2606. DOI: 10.1016/j.asr.2017.01.014.

Poluzzi, L., Tavasci, L., Corsini, F. et al. (2019). Low-cost GNSS sensors for monitoring applications. *Appl. Geomat.*. DOI: 10.1007/s12518-019-00268-5.

Romero-Andrade, R., Zamora-Maciel, A., Uriarte-Adrián, J.D J. et al. (2019). Comparative analysis of precise point positioning processing technique with GPS low-cost in different technologies with academic software. *Measurement: J. Int. Measurement Confederation*, 136. DOI: 10.1016/j.measurement.2018.12.100.

Romero-Andrade, R., Trejo-Soto, M.E., Vázquez-Ontiveros, J.R. (2021a). Sampling rate impact on Precise Point Positioning with a Low-Cost GNSS receiver. *Appl. Sci.*, 11, 17. DOI: 10.3390/app11167669.

Romero-Andrade, R., Trejo-soto, M.E., Vega-ayala, A. et al. (2021b). Positioning Evaluation of Single and Dual-Frequency Low-Cost GNSS Receivers Signals Using PPP and Static Relative Methods in Urban Areas. *Appl. Sci.*, 1–17. DOI: 10.3390/app112210642.

Saastamoinen, J. (1973). Contributions to the theory of atmospheric refraction. *Bulletin Géodésique* (1946-1975), 107(1), 13–34.

Sioulis, A., Tsakiri, M., and Stathas, D. (2015). Evaluation of low cost, high sensitivity GNSS receivers based on the ISO RTK standards. *Int. J. Geomat. Geosci.*, 6(2), 1597–1606.

Structural Deformation Surveying (EM 1110-2-1009) (2018).

Szostak-Chrzanowski, A. (2006). Interdisciplinary approach to deformation analysis in engineering, mining, and geosciences projects by combining monitoring surveys with deterministic modeling. Part II. *Tech. Sci.*, 9, 147–172.

Takasu, T. (2013). RTKLIB 2.4.2 Manual (Issue C).

Tétreault, P., Kouba, J., Héroux, P. et al. (2005). CSRS-PPP: An internet service for GPS user access to the Canadian Spatial Reference frame. Geomatica, 59(1), 17–28.

Teunissen, P.J.G. (2020). GNSS Precise Point Positioning. In Position, Navigation, and Timing Technologies in the 21st Century (pp. 503–528). John Wiley & Sons, Ltd. DOI: 10.1002/9781119458449.ch20.

Tsakiri, M., Sioulis, A., and Piniotis, G. (2017). Compliance of low-cost, single-frequency GNSS receivers to standards consistent with ISO for control surveying. *Int. J. Metrol. Quality Eng.*, 8. DOI: 10.1051/ijmqe/2017006.

Tsakiri, M., Sioulis, A., and Piniotis, G. (2018). The use of low-cost, single-frequency GNSS receivers in mapping surveys. *Sur. Rev.*, 50(358), 46–56. DOI: 10.1080/00396265.2016.1222344.

Tunini, L., Zuliani, D., and Magrin, A. (2022). Applicability of Cost-Effective GNSS sensor for crustal deformation studies. *Sensors*, 22, 350. https://pubmed.ncbi.nlm.nih.gov/35009892/.

Ublox. (2022). u-center 22.07, p. 1-15.

Vázquez-Ontiveros, J.R., Martinez-Felix, C.A., Vazquez-Becerra, G.E. (2022). Monitoring of local deformations and reservoir water level for a gravity type dam based on GPS observations. *Adv. Space Res.*, 69, 319–330. DOI: 10.1016/j.asr.2021.09.018.

Vázquez-Ontiveros, J.R., Ruiz-Armenteros, A.M., de Lacy-Pérez de los Cobos, M.C. et al. (2023). Risk Evaluation of the Sanalona Earthfill Dam Located in Mexico Using Satellite Geodesy Monitoring and Numerical Modeling. *Remote Sens.*, 15(819), 1–22. DOI: 10.3390/rs15030819.

Wielgocka, N., Hadas, T., Kaczmarek, A. et al. (2021). Feasibility of using low-cost dual-frequency gnss receivers for land surveying. *Sensors*, 21(6), 1–14. DOI: 10.3390/s21061956.

Wu, J.T., Wu, S.C., Hajj, G.A. et al. (1992). Effects of antenna orientation on GPS carrier phase. *Geod*, 18(2).

Xue, C., Psimoulis, P., Horsfall, A. et al. (2022). Assessment of the accuracy of low-cost multi-GNSS receivers in monitoring dynamic response of structures. *Appl. Geomat.* DOI: 10.1007/s12518-022-00482-8.

Yigit, C.O., Alcay, S., and Ceylan, A. (2016). Displacement response of a concrete arch dam to seasonal temperature fluctuations and reservoir level rise during the first filling period: evidence from geodetic data. *Geomat. Nat. Hazards Risk*, 7(4), 1489–1505. DOI: 10.1080/19475705.2015.1047902.

Zamora-Maciel, A., Romero-Andrade, R., Moraila-Valenzuela, C.R. et al. (2020). Evaluación de receptores GPS de bajo costo de alta sensibilidad para trabajos geodésicos . Caso de estudio : línea base geodésica. *Ciencia Ergo-Sum*, 27, 10–17. DOI: 10.30878/ces.v27n1a5.

Zhao, L., Yang, Y., Xiang, Z. et al. (2022). A Novel Low-Cost GNSS Solution for the Real-Time Deformation Monitoring of Cable Saddle Pushing : A Case Study of Guojiatuo Suspension Bridge. *Remote Sens.*, 14(5174). DOI: 10.3390/rs14205174.